Uncoupling the ATPase Activity of the *N*-Ethylmaleimide Sensitive Factor (NSF) from 20S Complex Disassembly[†]

Elena A. Matveeva,[‡] Andrew P. May,[§] Ping He,[‡] and Sidney W. Whiteheart*,[‡]

Department of Molecular and Cellular Biochemistry, Chandler Medical Center, University of Kentucky College of Medicine, Lexington, Kentucky 40536, and Department of Structural Biology, Stanford University School of Medicine, Stanford, California 94305

Received August 1, 2001; Revised Manuscript Received September 17, 2001

ABSTRACT: The *N*-ethylmaleimide sensitive factor (NSF) plays a critical role in intracellular trafficking by disassembling soluble NSF attachment protein receptor (SNARE) complexes. The NSF protomer consists of three domains (NSF-N, NSF-D1, and NSF-D2). Two domains (NSF-D1 and NSF-D2) contain a conserved ∼230 amino acid cassette, which includes a distinctive motif termed the second region of homology (SRH) common to all ATPases associated with various cellular activities (AAA). In hexameric NSF, several SRH residues become trans elements of the ATP binding pocket. Mutation of two conserved arginine residues in the NSF-D1 SRH (R385A and R388A) did not effect basal or soluble NSF attachment protein (SNAP)-stimulated ATPase activity; however, neither mutant underwent ATP-dependent release from SNAP−SNARE complexes. A trans element of the NSF-D2 ATP binding site (K631) has been proposed to limit the ATPase activity of NSF-D2, but a K631D mutant retained wild-type activity. A mutation of the equivalent residue in NSF-D1 (D359K) also did not affect nucleotide hydrolysis activity but did limit NSF release from SNAP−SNARE complexes. These trans elements of the NSF-D1 ATP binding site (R385, R388, and D359) are not required for nucleotide hydrolysis but are important as nucleotide-state sensors. NSF-N mediates binding to the SNAP−SNARE complex. To identify the structural features required for binding, three conserved residues (R67, S73, and Q76) on the surface of NSF-N were mutated. R67E completely eliminated binding, while S73R and Q76E showed limited effect. This suggests that the surface important for SNAP binding site lies in the cleft between the NSF-N subdomains adjacent to a conserved, positively charged surface.

The *N*-ethylmaleimide sensitive factor (NSF)[1] was one of the first proteins identified to play a role in vesicular trafficking (*1*). Since that time, NSF has been shown to be required for almost every intracellular trafficking event in the cell (reviewed in refs *2* and *3*). The membrane fusion events central to vesicular trafficking are facilitated by the formation of a heterotrimeric or heterotetrameric complex of integral membrane proteins called soluble NSF attachment protein receptors (SNAREs; reviewed in refs *4*−*6*). NSF acts as a chaperone or "protein unfoldase" by disassembling complexes of SNARE proteins once membrane fusion has been completed (reviewed in refs *3*, *7*, and *8*). NSF can also affect the disassembly and rearrangement of complexes that do not contain the full complement of SNARE proteins (*9*−*11*). Adaptor proteins called soluble NSF attachment proteins (SNAPs) bind NSF to SNARE complexes (*12*, *13*), forming the so-called 20S complex (*14*, *15*). Once the SNAP−SNARE complex is bound, interactions with SNAPs stimulate the ATPase activity of NSF and promote SNARE complex disassembly (*16*, *17*).

NSF is a homohexameric protein (*18*) whose protomers can be divided into three domains (*19*): an N-terminal domain (NSF-N, a.a. 1−205), and two ATP binding domains (NSF-D1, a.a. 206−477; NSF-D2, a.a. 478−744). Studies show that each domain distinctly contributes to the overall function of the NSF protein: NSF-N is required for SNAP binding; NSF-D1, the first ATP binding domain, is required for SNARE complex disassembly; and NSF-D2 is required for hexamerization (*17*, *20*−*23*). As compared to NSF-D2, NSF-D1 has a lower affinity for ATP and accounts for the majority of NSF basal and SNAP-stimulated ATPase activity (*17*, *22*, *23*). One potential reason for the low hydrolytic activity of NSF-D2 may be Lys631, which interacts directly with the γ-phosphate of ATP bound to an adjacent protomer in the NSF-D2 hexamer (*24*, *25*). This residue, which is substituted for asparatic acid in NSF-D1, is proposed to disrupt the charge distribution during ATP hydrolysis (*24*, *25*).

Both of the ATP binding domains of NSF contain the 230−250 amino acid motif that is the hallmark of the AAA family of cellular ATPases (*26*−*28*). AAA proteins use ATP

[†] This work was supported by the National Heart, Lung and Blood Institute of the National Institutes of Health (Grant HL56652), by the Ohio Valley Affiliate of the American Heart Association (Grant 0150841B to S.W.W.), and by a Wellcome Trust International Prize Traveling Research Fellowship (to A.P.M.).

* To whom correspondence should be addressed. E-mail whitehe@pop.uky.edu. Fax: 859-323-1037. Phone: 859-257-4882.

[‡] University of Kentucky College of Medicine.

[§] Stanford University School of Medicine.

[1] Abbreviations: NSF, *N*-ethylmaleimide sensitive factor; SNAP, soluble NSF attachment protein; SNARE, SNAP receptor; SRH, second region of homology; AAA, ATPases associated with various cellular activities; VCP, valosin-containing protein; VAT, VCP-like ATPase from *Thermoplasma acidophilium*; DPBB, double ψ β barrel; EM, electron microscopy.

10.1021/bi015632s CCC: $22.00
Published on Web 12/14/2001

hydrolysis to carry out a wide range of cellular processes, from facilitating membrane fusion to protein degradation (reviewed in ref *29*). As with other nucleotide-binding motifs, the AAA sequence contains both Walker A and B motifs, which make up the core of the ATP binding site. Mutational analysis shows that these motifs are important for both nucleotide binding and hydrolysis (*17*, *20*, *21*). The AAA domains of a number of proteins have a very similar overall structure. NSF-D2 (*24*, *25*), p97/VCP-D1 (*30*), HsIU (*31*, *32*), RuvB (*33*), and the clamp loader complex *(34)* all have an α/β subdomain that contains the nucleotide binding pocket and a C-terminal helical subdomain that lies close to the nucleotide-binding pocket. One unique feature of the AAA cassette is the so-called second region of homology (SRH). The SRH is a highly conserved region of ~18 amino acids located within the nucleotide-binding subdomain (*27*, *28*). Residues at the N-terminal end of the SRH are in close proximity (<8 Å; see ref *30*) to the phosphates of the bound nucleotide. Mutation of one of these residues Thr394 in Sec18p to a proline eliminates ATPase activity (*35*). Several AAA proteins are hexameric (*36*) and, in that state, observed in the crystal structures of NSF-D2 (*24*, *25*), HsIU (*31*, *32*) and p97-D1 (*30*), some of the C-terminal residues of the SRH form part of the interprotomer interface. Because of this trans arrangement, these residues become part of the nucleotide-binding pocket of an adjacent protomer and are proposed to function in nucleotide binding and hydrolysis or in nucleotide-state sensing *(34, 37−39)*.

NSF-N is required for SNAP binding. Truncation mutants lacking NSF-N are hexameric and have basal ATPase activity but fail to bind SNAP−SNARE complexes (*22*, *40*). NSF-N (*41*, *42*) and its yeast equivalent Sec18-N (*43*) are composed of two subdomains connected by a linker of variable length. The first subdomain (N_A, 1−83) is made up of six β strands arranged in a barrel with two "ψ loops" containing short α helices (α1 and α2) extending over the top. This so-called double ψ β barrel (DPBB) is found in several other proteins and the ψ loops have been associated with substrate binding (*44*). The second subdomain (N_B) is composed of four β strands wrapped around a single amphipathic α helix. Interestingly, despite limited sequence conservation, there is significant structural similarity between NSF-N and the analogous N domains of both p97/VCP (*30*) and VAT (*45*).

Because NSF-N is important for SNAP−SNARE binding, structural analysis has focused on identifying regions that could serve as binding sites for the acidic C terminus of SNAPs (*42*, *46*, *47*). Three "grooves" of sufficient size are present in NSF-N (*42*). Given that ψ loops of DPBB domains are often involved in ligand binding (*44*), it is of note that the α2 helix, in the second ψ loop of NSF-N_A, contains a highly conserved arginine residue, Arg67. The Arg67 side chain is exposed on the surface that bounds one side of a surface groove on NSF-N, which has been proposed to be the likely SNAP binding site (*42*). The analogous groove in p97-N also contains an arginine residue (Arg89) equivalent to Arg67 in NSF.

The experiments presented here begin to address which specific regions of the protomer are important for three aspects of NSF activity: (1) nucleotide hydrolysis, (2) SNAP−SNARE complex binding, and (3) NSF−SNAP−SNARE complex disassembly.

EXPERIMENTAL PROCEDURES

Reagents. ATP was obtained from Boehringer Mannheim Biochemicals (Indianapolis, IN). [α^{32}P]-ATP (800 Ci/mmol) was from ICN (Costa Mesa, CA). Pure nitrocellulose membranes (0.2 μm) for immunoblotting were purchased from Schleicher & Schuell (Keene, NH). Horseradish peroxidase conjugated anti-immunoglobulin secondary antibodies were from Sigma (St. Louis, MO), and SuperSignal chemiluminescent substrate was purchased from Pierce (Rockford, IL). Polyethyleneimine cellulose plates for thin-layer chromatography were from Selecto Scientific (Norcross, GA). Glutathione, immobilized on cross-linked 4% beaded agarose, was from Sigma. All chemicals were of reagent grade.

Production and Purification of Recombinant Proteins and Mutants. Wild-type His_6-NSF and His_6-NSF mutants were produced as recombinant proteins in *Escherichia coli* and purified as described (*22*). Site-directed mutagenesis was accomplished using the QuickChange kit according to manufacturer's instructions (Stratagene, La Jolla, CA), and mutations were confirmed by dideoxy nucleotide sequencing. Recombinant His_6-α-SNAP, His_6-SNAP-25, and GST-syntaxin 1 (cytoplasmic domain) were prepared as previously described (*9*, *10*, *22*). Protein concentrations were measured with the BioRad protein assay reagent (BioRad, Hercules, CA) using ovalbumin as a standard.

Gel Electrophoresis and Immunoblotting. Sodium dodecyl sulfate−polyacrylamide gel electrophoresis (SDS−PAGE) was performed under reducing conditions on 10% slab gels in a discontinuous buffer system (*48*). Western blotting onto nitrocellulose was performed according to standard techniques (*22*) using 5% powdered milk in Tris-buffered saline to block nonspecific interactions. Horseradish peroxidase conjugated anti-mouse immunoglobulin antibodies were used as secondary reagents. SuperSignal substrate was used to visualize the immunodecorated antigens using X-OMAT X-ray film (Eastman Kodak Co., Rochester, NY), and the film was developed using a medical film processor Konica QX-70 (Picker, Cleveland, OH).

SNAP−SNARE Complex Binding Assay. The complex formation procedure was modified from previously described methods (*17*). Briefly, GST-syntaxin 1 was incubated with preswollen, glutathione−agarose beads (100 μg of protein/100 μL of beads) at 4 °C in phosphate-buffered saline with 0.01% (v/v) Tween 20, 0.1% (v/v) β-mercaptoethanol, and 2 mM EDTA. After 1 h, the beads were washed four times (0.5 mL each) in the same buffer, and then equal volumes of the beads (and therefore an equal amount of SNARE complexes) were aliquotted into the reaction tubes. Complex formation reactions were performed in a final volume of 500 μL containing 15 μL of beads with GST-syntaxin 1 in binding buffer (20 mM HEPES/KOH (pH 7.4), 250 mM imidazole, 150 mM potassium acetate, 5 mM EGTA, 2.5 mM AMP−PNP, 5 mM $MgCl_2$, 1% (w/v) glycerol, 1% (w/v) Triton X-100, and 10% (w/v) ovalbumin) and saturating amounts of α-SNAP, SNAP-25, and wild-type or mutant NSF. After 3 h at 4 °C, the beads were washed five times (1 mL each) with binding buffer without ovalbumin. The bound proteins were eluted with an SDS−PAGE sample buffer and analyzed by western blotting using the anti-NSF monoclonal antibody 2E5 (*20*), which equally detects both mutant and

wild-type NSF. The binding of wild-type and mutant NSF was always SNAP-dependent.

To measure the release of bound NSF from SNAP−SNARE complexes, the complexes, were preformed on the GSH−agarose beads and incubated for 45 min at 25 °C in a binding buffer with the AMP−PNP replaced with 5 mM ATP. The beads were recovered by centrifugation, and the bound proteins were eluted with an SDS−PAGE sample buffer. The dissociated proteins, in the supernatant, were precipitated with 10% (w/v) trichloroacetic acid, and both bound and released samples were analyzed by western blotting.

ATPase Assay of NSF. ATPase assays were performed as a modification of previously described methods (*10*) using [α^{32}P]-ATP in a buffer containing 25 mM Tris HCl (pH 7.6), 100 mM KCl, 0.5 mM 1,4-dithiothreitol, 1 mM $MgCl_2$, 1% glycerol, 1 mM ATP, 10 μCi of [α^{32}P]-ATP, and 10 μg of wild-type or mutant NSF. To measure the effect of SNAP−SNARE complexes on wild-type or mutant NSF, ATPase reaction mixes were added directly to preformed SNAP−SNARE complexes and then incubated at 25 °C. After incubation, aliquots (2 μL) of each reaction were spotted on a polyethyleneimine thin-layer plate and chromatographed in 0.7 M LiCl and 1 M acetic acid. Plates were dried and then analyzed using a PhosphoImager from Molecular Dynamics (Sunnyvale, CA). ATPase activity was measured by determining the percent of [α^{32}P]-ADP produced relative to the total nucleotide present. In none of the reactions was any [α^{32}P]-AMP produced. The binary syntaxin 1−SNAP-25−SNARE complex was used in these experiments because it had been previously shown to cause maximal stimulation of the ATPase activity of NSF in these assays (*10*).

RESULTS AND DISCUSSION

Production of Recombinant NSF and Mutants. Three specific regions were examined by mutagenesis to determine their role in NSF activity. The first two are predicted to function in nucleotide hydrolysis. The third region has been proposed to be important for SNAP−SNARE binding. For region 1, on the basis of its proximity to the γ-phosphate of the ATP bound by an adjacent protomer in the NSF-D2 hexamer, Lys631 is predicted to disrupt charge distribution during γ-phosphate cleavage and therefore limit ATP hydrolysis by NSF-D2 (*24*, *25*). Conversely, the equivalent residue in NSF-D1 (Asp359) is proposed to have a positive effect on nucleotide hydrolysis (*37*). K631D and D359K mutants were created to determine the effect these residues have on nucleotide hydrolysis and NSF function. For region 2, two highly conserved arginine residues, present in the C-terminus of SRH of most AAA proteins, are important for both nucleotide hydrolysis and protease activity of bacterial FtsH (*38*). To determine the role of the equivalent residues in NSF, Arg385 and Arg388 were each changed to alanine. A double mutant (D359K−R385A) was produced to determine if a loss of one positive charge in the ATP binding site could be compensated for by the addition of a second in a proximal position. For region 3, the ψ loops of DPBB domains often contain residues with functional importance (*44*). In NSF-N, the second loop of NSF-N_A contains a highly conserved arginine residue (Arg67) that lies close to one of the surface grooves which is proposed to participate in SNAP binding (*42*). Mutagenesis of Arg67 along with two other nearby highly conserved residues (Ser73 and Gln76; see Figure 5C) was undertaken, and the resulting mutants were tested for SNAP−SNARE complex binding.

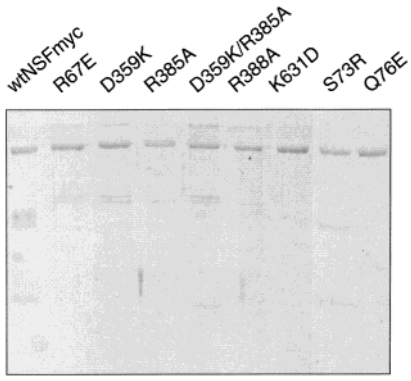

FIGURE 1: Recombinant protein preparations. Wild-type and mutant NSF proteins were expressed in *E. coli* and purified sequentially on Ni^{2+}-NTA agarose and Superose-6 columns. Each lane contains 5 μg of the indicated protein preparation. The 10% SDS−PAGE gel was stained with Coomassie Brilliant Blue.

Recombinant NSF and the point mutants were produced in *E. coli* as previously described (*20*, *22*). In each case, the proteins were initially purified by Ni^{2+}-NTA-agarose affinity chromatography, concentrated, and then further purified by sizing chromatography on Superose 6 (Figure 1). This second purification step assured the oligomeric nature of all recombinant proteins. Wild-type NSF and all mutant NSF proteins showed the same fractionation profile on Superose 6 (data not shown).

Basal and Stimulated ATPase Activity. Previous studies demonstrated that NSF has a low basal ATPase activity (4 mmol/mg/min (*19*)), which is stimulated 2−10-fold by the addition of SNAP−SNARE complexes (*10*, *16*, *23*). The mutant proteins were tested to determine if they had basal ATPase activity and whether SNAP−SNARE complexes could stimulate that activity. Basal ATPase activity was detected for each of the mutants tested, and it did not significantly differ from that of wild-type NSF (Figure 2A). The lack of increase in basal ATPase activity for the K631D mutant suggests that Lys631 is not solely responsible for the catalytic inactivity of NSF-D2. Because any increase in nucleotide hydrolysis by NSF-D2 could be masked by the higher activity of NSF-D1, the same mutation (K631D) was made in isolated NSF-D2. The mutant domain was oligomeric, migrating as did wild-type NSF-D2 on sizing chromatography, but there was no detectible increase in ATP hydrolysis activity (data not shown). In the converse experiment, a lysine residue placed in the analogous position (D359) of NSF-D1 had little significant effect on ATPase activity. Unexpectedly, the single mutation of either Arg385 or Arg388 (in the SRH) or the double mutation of Arg385 and Asp359 had no significant effect on basal ATPase activity. As expected, none of the mutations made in NSF-N affected basal ATPase activity (Figure 2A and data not shown).

The binary SNARE complex of syntaxin and SNAP-25 together with α-SNAP was previously shown to provide maximal stimulation of NSF ATPase activity (*10*). When this complex was added to the ATPase assays, each of the mutants, except R67E, showed a 5−6-fold increase in

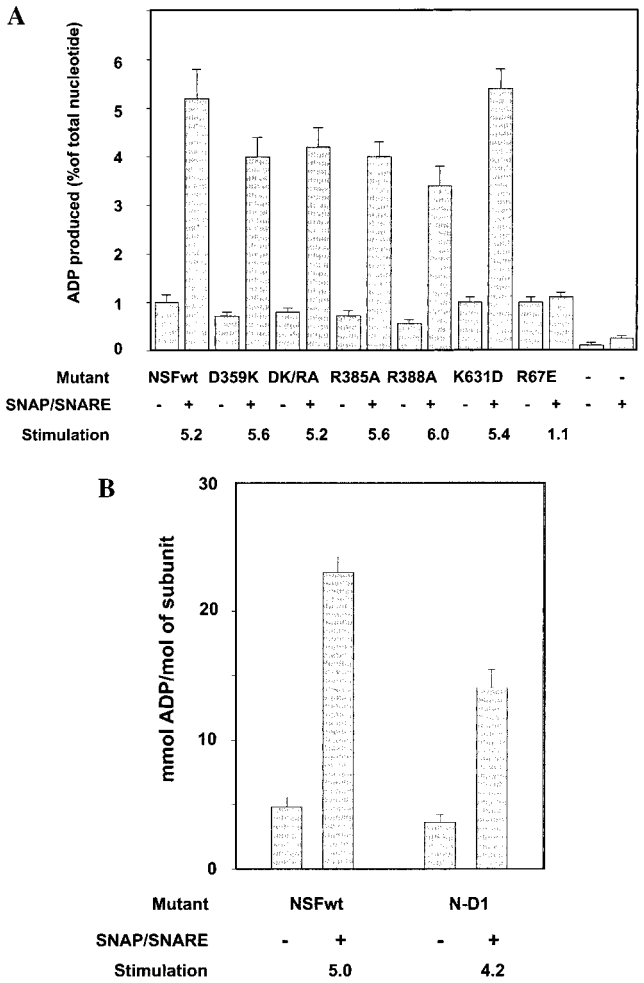

FIGURE 2: Basal and SNAP−SNARE-stimulated ATPase activities of wild-type and mutant NSF. In panel A, SNAP−SNARE complexes were formed as described in Experimental Procedures using 15 μL of GSH−agarose beads, 20 μg of GST-Syntaxin 1, and saturating amounts of His_6-αSNAP and His_6-SNAP-25. Basal and stimulated ATPase activities were measured for wild-type or mutant (10 μg) in the absence (−) or presence (+) of complex at 25 °C for 10 min in reaction buffer (total volume of 50 μL). The amount of [α^{32}P]-ADP produced is expressed as a percentage of the total nucleotide present in the reaction. The fold increases in ATPase activity (stimulation) were calculated by dividing the SNAP−SNARE-stimulated ATPase activity by the basal ATPase activity of NSF. Panel B shows the basal and SNAP−SNARE-stimulated ATPase activities for hexameric NSF and monomeric NSF-N-D1. Basal and SNAP−SNARE-stimulated ATPase activities were measured as in panel A. The amount of [α^{32}P]-ADP produced in 10 min at 25 °C is normalized to moles of protomer present.

ATPase activity, which was comparable to wild-type NSF. The R67E mutant failed to bind to the SNAP−SNARE complex and, therefore, was not stimulated (see Figure 4). The ATPase activity of all mutants was inhibited by prior treatment with NEM (5 mM for 30 min on ice, data not shown). The SNAP−SNARE complex on its own showed only background levels of nucleotide hydrolysis (Figure 2A, last set of lanes).

The observation that each mutant had apparently normal ATPase activity suggests that D359 and the arginine residues at the C-terminal end of the SRH have no significant effect on ATP hydrolysis by NSF-D1. This is surprising when compared to the bacterial AAA protein FtsH, where mutation of equivalent residues has a dramatic effect on ATPase activity (*38*). In those studies, it was proposed that the arginine residues act in trans on the ATP bound by the adjacent protomer to assist in nucleotide hydrolysis. Consistent with this, monomeric FtsH does not have detectable ATPase activity (*38*). For NSF, this is apparently not the case. To address this point further, we examined a monomeric form of NSF, NSF-N-D1. Shown in Figure 2B, NSF-N-D1 has basal ATPase activity as previously reported (*22*). The ATPase activity increased by 4-fold upon addition of SNAP−SNARE complexes. These two experiments suggest that, for NSF, the trans contributions of the adjacent subunit to the ATP binding site may not be required for nucleotide hydrolysis. These data show that the structures responsible for basal ATPase activity are contained entirely within the N-D1 fragment and most likely do not require oligomerization. It is, however, possible that NSF-N-D1 oligomerizes when bound and stimulated by SNAP−SNARE complexes but that no stable oligomer has been detected as free in solution (*20*, *22*). Further experimentation will be required to determine if NSF-N-D1 can oligomerize when bound to SNAP−SNARE complexes and whether those interactions are sufficient to affect ATP hydrolysis.

SRH Mutants Fail to Release from SNAP−SNARE Complex. Because NSF-N-D1 has ATPase activity but does not mediate membrane trafficking (*22*), it is clear that other enzymatic properties are also required for NSF function. We next examined the ability of NSF and the mutants to bind to and to release from the SNAP−SNARE complex in an ATPase-dependent manner. For these experiments, wild-type or mutant NSF was incubated with preformed SNAP−SNARE complexes in the presence of a nonhydrolysable ATP analogue (AMP−PNP). Binding was evaluated by coprecipitation of NSF with the SNARE fusion protein (GST-syntaxin). Release was evaluated by measuring the appearance of NSF in the supernatant after incubation of the NSF−SNAP−SNARE complex in the presence of ATP. In Figure 3, ∼60% of the wild-type NSF, prebound to the SNAP−SNARE complex, was released into the supernatant when incubated with ATP. This behavior was also seen with the NSF-D2 mutant, K631D. Consistent with previous reports (*22*), the E329Q mutant of NSF-D1, shown to be defective in ATP hydrolysis, did bind to SNAP−SNARE complexes but was not released into the supernatant upon addition of ATP. This mutant is frozen in the ATP-bound state and is, therefore, unable to initiate the ATPase-dependent conformational changes required for release from SNAP−SNARE complexes. Similar behavior was seen with the D358K mutant, the two SRH mutants (R385A and R388A), and the double mutant (D359K/R385A). The two, R-A mutants have the more severe defect, but none of the four mutants were able to release from the SNAP−SNARE complex to the extent of the wild-type NSF (Figure 3). The D359K, R385A, R388A, and D359K/R385A mutants clearly bound to the SNAP−SNARE complex, albeit to differing extents (Figure 3). This indicates that the mutants were able to attain the ATP-dependent SNAP−SNARE-binding-competent conformation but also suggests that the efficiency of conversion to that conformation may be affected by the mutations. Further quantitative binding studies will be required to determine the binding constants for these interactions.

In summary, the D359K, R385A, R388A, and D359K/R385A mutants can attain the conformation required for SNAP−SNARE binding and can hydrolyze nucleotides.

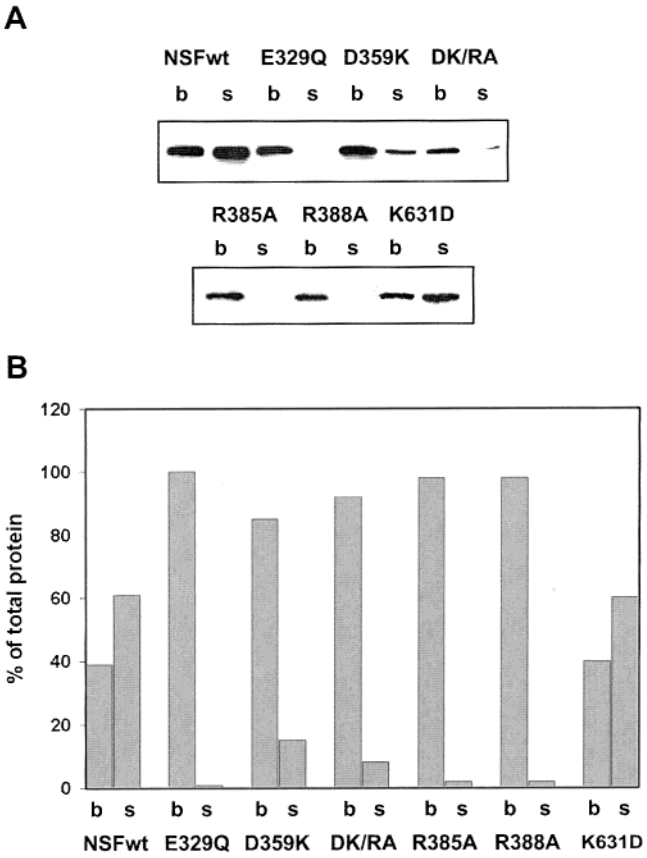

FIGURE 3: ATPase-dependent release of NSF and mutants from SNAP−SNARE complexes. Preformed NSF−SNAP−SNARE complexes were incubated for 45 min at 25 °C in the presence of 5 mM ATP. The bound (b) and released (s) proteins were analyzed by western blotting using the 2E5 monoclonal antibody as shown in panel A and quantified by densitometry as shown in panel B. The data presented are representative of three distinct experiments.

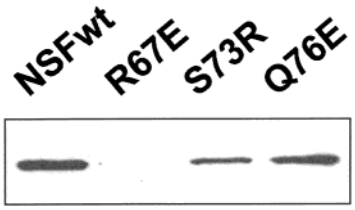

FIGURE 4: Binding of NSF-N domain mutants to SNAP−SNARE complexes. SNAP−SNARE complexes were formed as described in Experimental Procedures from GST-Syntaxin 1, α-SNAP, SNAP-25, and NSF or mutant in the presence of 2.5 mM AMP−PNP. The bound proteins were eluted with an SDS−PAGE sample buffer and analyzed by western blotting using the 2E5 monoclonal antibody. The data presented are representative of three distinct experiments.

However, they were unable to initiate or propagate the ATP-dependent conformational change(s) required for release from the SNAP−SNARE complex. This deficiency could be the result of a lack of coordination between protomers as these residues most likely act in trans. Such coordination is apparently important because ATP binding by all six copies of NSF-D1 is required for NSF activity (*20*).

SNAP Binding Regions of NSF-N. Arg67 is one of the most highly conserved residues in the N domains of all known NSF orthologues (*3*). This residue lies in the middle of the α2 helix, which is part of the second ψ loop of both NSF and Sec18p. Arg67 is also adjacent to a putative SNAP binding region (*42*). Mutations were made at three conserved positions on NSF-N: R67E, S73R, and Q76E (see Figure 5C). These mutant proteins were tested for their ability to bind to the SNAP−SNARE complex (Figure 4). The two mutants S73R and Q76E did bind SNAP−SNARE complexes, though, with apparently lower efficiency than did wild-type NSF. This suggests that this region of the NSF-N surface may play a limited role in SNAP−SNARE complex binding. Mutation of Arg67, however, completely eliminated binding. All three mutants were hexameric and retained wild-type levels of basal ATPase activity (Figure 2A and data not shown).

The sequence and structural conservation of Arg67 in NSF orthologues and other AAA proteins (i.e., p97/VCP and VAT) suggest that this residue could play an important functional role. Arg67 is positioned in the middle of the α2 helix of NSF-N_A (Figure 5C) and similarly in p97/VCP-N_A (*30*) and VAT-N_A (*45*) such that the side chain is surface-exposed and proximal to a surface groove proposed as a potential ligand binding site (*41*−*43*). A positive charge on the binding surface may function as a reference point for binding, especially for ligands with significant negative charges such as α- and β-SNAP. Consistent with the effect of the Arg67 mutation, a temperature-sensitive mutation of yeast NSF (Sec18p), Sec18−1, results in the replacement of Gly95 with aspartic acid (*41*). Gly95 in Sec18p is equivalent to Ala70 in NSF, and a change of this residue to aspartic acid would disrupt the positioning of the α2 helix, presumably resulting in a disruption of this surface region. The surface region containing the α2 helix and, in particular, the highly conserved Arg67 is clearly required for SNAP−SNARE binding and, hence, for stimulation of NSF ATPase activity (Figure 2A). Further mutagenesis will be required to more fully define the boundaries of the SNAP binding site on NSF-N.

Mechanistic Implications. Unfortunately, there is no detailed structural information available for NSF-N-D1. However, the structure of p97-N-D1 does provide insight into how the mutations discussed here could affect NSF function (see Figure 5). The surface containing the residue equivalent to Arg67 (Arg89 in p97/VCP) is inaccessible in the ADP-bound form of p97-N-D1 (*30*). In this nucleotide state, the interdomain linker (dark-brown ribbon in Figure 5A) buries the argnine residue into the p97N−p97D1 interface. In negatively stained EM images, the ADP-bound NSF hexamer has a barrel-like shape (*49*); therefore, NSF-N-D1 could adopt a conformation similar to that shown for ADP-bound p97-N-D1. The burial of Arg67 into the N-D1 interface would prevent the binding of SNAPs. With ATP bound, NSF exposes a cationic surface (*43*) and is competent to bind SNAPs (*17*, *22*). Negatively stained EM images of ATP-bound NSF suggest that the N domains can extend radially from the central barrel core (*49*). This arrangement demonstrates that NSF-N is on a flexible linker arm and is not tucked in alongside the NSF-D1 when NSF-D1 is in the ATP-bound state. As an additional point, one crystal form of NSF-N contains a trimeric assembly of protomers that has been proposed to have functional significance (*41*). In this configuration, the side chains of Arg67 are exposed on the surface of each protomer where they would be accessible for SNAP binding. All of these data are consistent with the model whereby NSF binds to SNAPs, when in the ATP-

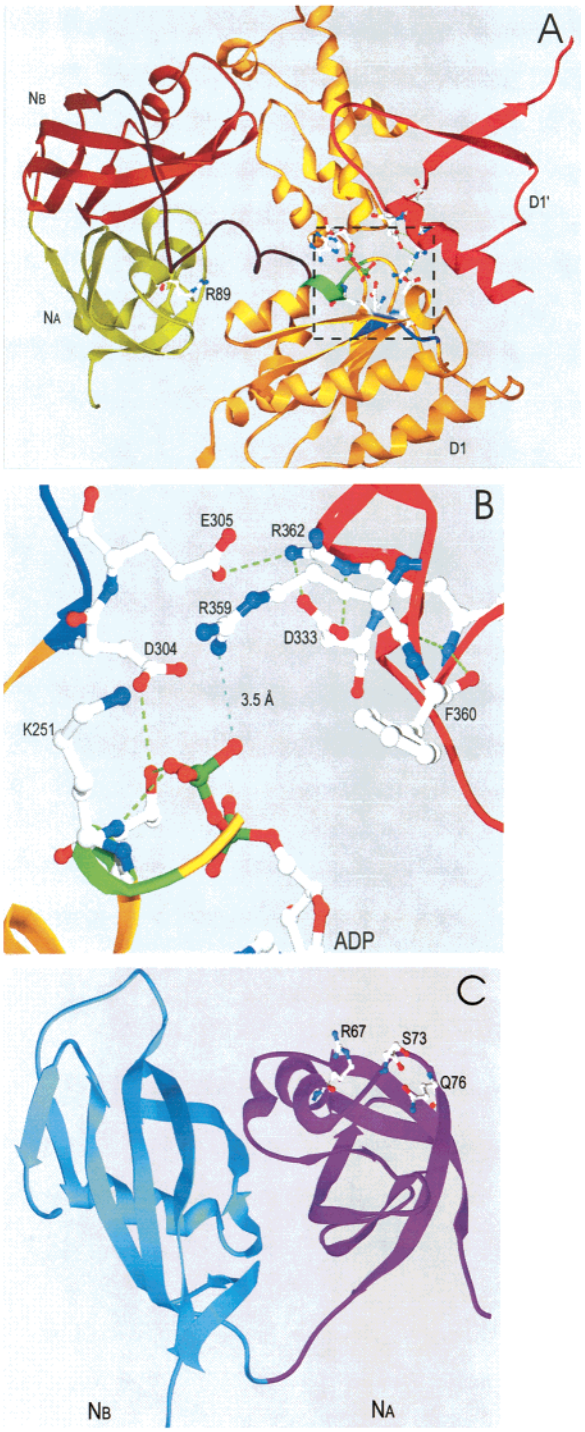

FIGURE 5: Positions of the p97-N-D1 equivalents to the residues mutated in NSF. Panel A shows a p97-N-D1 protomer (N_A in olive, N_B in brown, interdomain linker in dark brown, and D1 in yellow). The ribbon diagram of the p97-D1 domain, shown in yellow, is highlighted using green for the P loop and blue for the DEAD box. The residues of the SRH from the adjacent D1′ domain in the hexamer are denoted by the red ribbon. The arginine residue equivalent to NSF-Arg67 (R89) is marked in the p97-N_A domain. Panel B shows an expanded view of the nucleotide binding site depicted in the boxed region in panel A. This region has been rotated 180° relative to that shown in panel A. The p97 residues, equivalent to those mutated in NSF, are shown and are described in the text. Hydrogen bonds are shown as dotted green lines, and the dotted aqua line from the Arg359 to the ADP β-phosphate indicated the line used to measure the distance between the two atoms. Panel C shows the crystal structure of NSF-N. N_A is in magenta and N_B is in blue. These figures were generated using Swiss PDB viewer and rendered with PovRay.

bound conformation, because the surface containing Arg67 is exposed.

On the basis of the crystal structure of the ADP-bound form of p97 (Figure 5A,B), it is possible to see how some of the trans residues at the C terminus of the SRH might affect conformational changes through the hexamer. p97-Arg362 (equivalent to NSF-Arg388) is positioned so that it forms a salt bridge with p97-E305 (NSF-E329) from the adjacent protomer (Figure 5B). p97-Asp333 (NSF-Asp359) likely maintains the position of p97-Arg362 through two hydrogen bonds (Figure 5B). Mutation of either of these two residues would be expected to affect the formation of the salt bridge between E305 and Arg362 and could, therefore, disrupt nucleotide-dependent interprotomer contacts.

The role for p97-Arg359 (NSF-Arg385) is less apparent. On the basis of its proximity to the β-phosphate of ADP (3.5 Å; Figure 5B) and the potential effect that a γ-phosphate, from ATP, might have on the positioning of its side chain, p97-Arg359 could be responsive to the nucleotide bound. Both p97-Arg359 and p97-Phe360 have higher B factors than the surrounding residues (*30*) suggesting potential disorder or flexibility at those positions. In the clamp loader complex, a structurally equivalent arginine (Arg169 in sensor 1) has different conformations in each of the three γ subunits (*34*). Using crude modeling analysis, the authors suggest that a nucleotide bound to the γ-1 subunit would affect the conformation of the SRH in γ-2, resulting in an opening of the site for nucleotide binding. Binding of nucleotide to γ-2 would then induce a similar conformational change in the γ-3 subunit. Such analysis shows that this arginine in the SRH is positioned to be responsive to the nucleotide of one binding site and affects the conformation in the next. From the data presented in this paper, this arginine is not required for ATP hydrolysis by NSF, but it does play a role in the nucleotide-dependent disengagement of the NSF hexamer from the SNAP−SNARE complex.

While the C-terminal residues of the SRH appear to act in trans, the N-terminal residues appear to be cis elements of the nucleotide binding site. One highly conserved residue at the N terminus of the SRH (Thr394 in Sec18p, equivalent to Thr381 in NSF and Thr347 in p97) is important for nucleotide hydrolysis (*35*). Mutation of Thr394 to proline results in a dominant-negative form of Sec18p that cannot hydrolyze ATP. These data together with the data presented in this paper suggest that the N- and C-terminal residues of the SRH may play distinct roles in the mechanism of AAA proteins. The highly conserved SRH cassette may directly connect ATP hydrolysis at one nucleotide binding site and the structural changes of an adjacent ATP binding site. While this insight into the mechanisms of AAA proteins will be valuable in the design of future experiments and in the interpretation of structural analysis, it remains to be seen how widely applicable this mechanism will be in non-olgimeric AAA family members.

ACKNOWLEDGMENT

The authors specifically thank Dr. Teru Ogura and Dr. William I. Weis for their helpful discussions during the preparation of the manuscript. We thank the members of the Whiteheart laboratory and Dr. Susan Buhrow for their discussions and comments. We also thank Dr. Xiangdong

Zhang and Dr. Paul S. Freemont for making the coordinates for the p97-N-D1 structure available to us prior to their release.

REFERENCES

1. Block, M. R., Glick, B. S., Wilcox, C. A., Wieland, F. T., and Rothman, J. E. (1988) *Proc. Natl. Acad. Sci. U.S.A. 85*, 7852−6.
2. Woodman, P. G. (1997) *Biochim. Biophys. Acta 1357*, 155−72.
3. Whiteheart, S. W., Schraw, T. D., and Matveeva, E. A. (2001) *Int. J. Cytology 207*, 71−112.
4. Jahn, R., and Sudhof, T. C. (1999) *Annu. Rev. Biochem. 68*, 863−911.
5. Chen, Y. A., and Scheller, R. H. (2001) *Nat. Rev. Mol. Cell. Biol. 2*, 98−106.
6. Hay, J. C., and Scheller, R. H. (1997) *Curr. Opin. Cell Biol. 9*, 505−12.
7. Morgan, A., and Burgoyne, R. (1995) *Trends Cell Biol. 5*, 335−9.
8. May, A. P., Whiteheart, S. W., and Weis, W. I. (2001) *J. Biol. Chem. 276*, 21991−4.
9. Hanson, P. I., Otto, H., Barton, N., and Jahn, R. (1995) *J. Biol. Chem. 270*, 16955−61.
10. Matveeva, E., and Whiteheart, S. W. (1998) *FEBS Lett. 435*, 211−4.
11. Haynes, L. P., Barnard, R. J., Morgan, A., and Burgoyne, R. D. (1998) *FEBS Lett. 436*, 1−5.
12. Clary, D. O., and Rothman, J. E. (1990) *J. Biol. Chem. 265*, 10109−17.
13. Clary, D. O., Griff, I. C., and Rothman, J. E. (1990) *Cell 61*, 709−21.
14. Wilson, D. W., Whiteheart, S. W., Wiedmann, M., Brunner, M., and Rothman, J. E. (1992) *J. Cell Biol. 117*, 531−8.
15. Sollner, T., Whiteheart, S. W., Brunner, M., Erdjument-Bromage, H., Geromanos, S., Tempst, P., and Rothman, J. E. (1993) *Nature 362*, 318−24.
16. Morgan, A., Dimaline, R., and Burgoyne, R. D. (1994) *J. Biol. Chem. 269*, 29347−50.
17. Matveeva, E. A., He, P., and Whiteheart, S. W. (1997) *J. Biol. Chem. 272*, 26413−8.
18. Fleming, K. G., Hohl, T. M., Yu, R. C., Muller, S. A., Wolpensinger, B., Engel, A., Engelhardt, H., Brunger, A. T., Sollner, T. H., and Hanson, P. I. (1998) *J. Biol. Chem. 273*, 15675−81.
19. Tagaya, M., Wilson, D. W., Brunner, M., Arango, N., and Rothman, J. E. (1993) *J. Biol. Chem. 268*, 2662−6.
20. Whiteheart, S. W., Rossnagel, K., Buhrow, S. A., Brunner, M., Jaenicke, R., and Rothman, J. E. (1994) *J. Cell Biol. 126*, 945−54.
21. Sumida, M., Hong, R. M., and Tagaya, M. (1994) *J. Biol. Chem. 269*, 20636−41.
22. Nagiec, E. E., Bernstein, A., and Whiteheart, S. W. (1995) *J. Biol. Chem. 270*, 29182−8.
23. Steel, G. J., and Morgan, A. (1998) *FEBS Lett. 423*, 113−6.
24. Lenzen, C. U., Steinmann, D., Whiteheart, S. W., and Weis, W. I. (1998) *Cell 94*, 525−36.
25. Yu, R. C., Hanson, P. I., Jahn, R., and Brunger, A. T. (1998) *Nat. Struct. Biol. 5*, 803−11.
26. Erdmann, R., Wiebel, F. F., Flessau, A., Rytka, J., Beyer, A., Frohlich, K. U., and Kunau, W. H. (1991) *Cell 64*, 499−510.
27. Beyer, A. (1997) *Protein Sci. 6*, 2043−58.
28. Neuwald, A. F., Aravind, L., Spouge, J. L., and Koonin, E. V. (1999) *Genome Res. 9*, 27−43.
29. Patel, S., and Latterich, M. (1998) *Trends Cell Biol. 8*, 65−71.
30. Zhang, X., Shaw, A., Bates, P. A., Newman, R. H., Gowen, B., Orlova, E., Gorman, M. A., Kondo, H., Dokurno, P., Lally, J., Leonard, G., Meyer, H., van Heel, M., and Freemont, P. S. (2000) *Mol. Cells 6*, 1473−84.
31. Bochtler, M., Hartmann, C., Song, H. K., Bourenkov, G. P., Bartunik, H. D., and Huber, R. (2000) *Nature 403*, 800−5.
32. Sousa, M. C., Trame, C. B., Tsuruta, H., Wilbanks, S. M., Reddy, V. S., and McKay, D. B. (2000) *Cell 103*, 633−43.
33. Yamada, K., Kunishima, N., Mayanagi, K., Ohnishi, T., Nishino, T., Iwasaki, H., Shinagawa, H., and Morikawa, K. (2001) *Proc. Natl. Acad. Sci. U.S.A. 98*, 1442−7.
34. Jeruzalmi, D., O'Donnell, M., and Kuriyan, J. (2001) *Cell 106*, 429−41.
35. Steel, G. J., Harley, C., Boyd, A., and Morgan, A. (2000) *Mol. Biol. Cell 11*, 1345−56.
36. Vale, R. D. (2000) *J. Cell Biol. 150*, F13−20.
37. Neuwald, A. F. (1999) *Structure Fold Des. 7*, R19−23.
38. Karata, K., Inagawa, T., Wilkinson, A. J., Tatsuta, T., and Ogura, T. (1999) *J. Biol. Chem. 274*, 26225−32.
39. Karata, K., Verma, C. S., Wilkinson, A. J., and Ogura, T. (2001) *Mol. Microbiol. 39*, 890−903.
40. Wimmer, C., Hohl, T. M., Hughes, C. A., Muller, S. A., Sollner, T. H., Engel, A., and Rothman, J. E. (2001) *J. Biol. Chem. 276*, 29091−7.
41. May, A. P., Misura, K. M., Whiteheart, S. W., and Weis, W. I. (1999) *Nat. Cell Biol. 1*, 175−82.
42. Yu, R. C., Jahn, R., and Brunger, A. T. (1999) *Mol. Cells 4*, 97−107.
43. Babor, S. M., and Fass, D. (1999) *Proc. Natl. Acad. Sci. U.S.A. 96*, 14759−64.
44. Castillo, R. M., Mizuguchi, K., Dhanaraj, V., Albert, A., Blundell, T. L., and Murzin, A. G. (1999) *Structure Fold Des. 7*, 227−36.
45. Coles, M., Diercks, T., Liermann, J., Groger, A., Rockel, B., Baumeister, W., Koretke, K. K., Lupas, A., Peters, J., and Kessler, H. (1999) *Curr. Biol. 9*, 1158−68.
46. Barnard, R. J., Morgan, A., and Burgoyne, R. D. (1996) *Mol. Biol. Cell 7*, 693−701.
47. Barnard, R. J., Morgan, A., and Burgoyne, R. D. (1997) *J. Cell Biol. 139*, 875−83.
48. Laemmli, U. K. (1970) *Nature 227*, 680−5.
49. Hanson, P. I., Roth, R., Morisaki, H., Jahn, R., and Heuser, J. E. (1997) *Cell 90*, 523−35.

BI015632S